

**FHS PUBLIC ACCESS**

Author manuscript

*Stroke*. Author manuscript; available in PMC 2016 April 01.

Published in final edited form as:

*Stroke*. 2015 April ; 46(4): 982–988. doi:10.1161/STROKEAHA.114.008154.**Defining the Ischemic Penumbra using Magnetic Resonance Oxygen Metabolic Index****Hongyu An, DSc<sup>1,\*</sup>, Andria L. Ford, MD<sup>2,\*</sup>, Yasheng Chen, PhD<sup>1</sup>, Hongtu Zhu, PhD<sup>3</sup>, Rosana Ponisio, MD<sup>4</sup>, Gyanendra Kumar, MD<sup>2</sup>, Amirali Modir Shanechi, MD<sup>5</sup>, Naim Houry, MD<sup>2</sup>, Katie D. Vo, MD<sup>4</sup>, Jennifer Williams, RN<sup>6</sup>, Colin P. Derdeyn, MD<sup>4</sup>, Michael N. Diringer, MD<sup>1</sup>, Peter Panagos, MD<sup>7</sup>, William J. Powers, MD<sup>8</sup>, Jin-Moo Lee, MD, PhD<sup>2,4,†</sup>, and Weili Lin, PhD<sup>1,8,†</sup>**<sup>1</sup>Department of Radiology, University of North Carolina at Chapel Hill<sup>2</sup>Department of Neurology, Washington University, School of Medicine<sup>3</sup>Department of Biostatistics, University of North Carolina at Chapel Hill<sup>4</sup>Department of Radiology, Washington University, School of Medicine<sup>5</sup>Washington University School of Medicine<sup>6</sup>Barnes-Jewish Hospital Emergency Department<sup>7</sup>Department of Emergency Medicine, Washington University School of Medicine<sup>8</sup>Department of Neurology, University of North Carolina at Chapel Hill**Abstract**

**Background and Purpose**—Penumbral biomarkers promise to individualize treatment windows in acute ischemic stroke. We used a novel MRI approach which measures oxygen metabolic index (OMI), a parameter closely related to PET-derived cerebral metabolic rate of oxygen utilization, to derive a pair of ischemic thresholds: (1) an irreversible-injury threshold which differentiates ischemic core from penumbra and (2) a reversible-injury threshold which differentiates penumbra from tissue not-at-risk for infarction.

**Methods**—Forty acute ischemic stroke patients underwent MRI at three time-points after stroke onset: < 4.5 hours (for OMI threshold derivation), 6 hours (to determine reperfusion status), and 1 month (for infarct probability determination). A dynamic susceptibility contrast method measured CBF, and an asymmetric spin echo sequence measured OEF, to derive OMI (OMI=CBF\*OEF). Putative ischemic threshold pairs were iteratively tested using a computation-intensive method to derive infarct probabilities in three tissue groups defined by the thresholds (core, penumbra, and not-at-risk tissue). An optimal threshold pair was chosen based on its ability to predict: infarction

<sup>†</sup>Correspondence author: Weili Lin, PhD, University of North Carolina, 106 Mason Farm Road, Campus Box 7515, Chapel Hill, NC 27599, [weili\\_lin@med.unc.edu](mailto:weili_lin@med.unc.edu), Telephone: (919) 843-8120, Fax: (919) 843-4438; Jin-Moo Lee, M.D., Ph.D., Washington University, School of Medicine, Department of Neurology, 600 South Euclid Avenue, Campus Box 8111, Saint Louis, Missouri 63110, [leejm@neuro.wustl.edu](mailto:leejm@neuro.wustl.edu), Telephone: (314) 362-7382, Fax: (314) 747-3342.

\*Contributed equally

**Disclosures:** Hongyu An receives research support from Siemens. Colin Derdeyn receives modest consulting fees from Penumbra, Inc. and MicroVention. William Powers received honoraria for two invited continuing medical education stroke lectures.

in the core, reperfusion-dependent survival in the penumbra, and survival in not-at-risk tissue. The predictive abilities of the thresholds were then tested within the same cohort using a 10-fold cross-validation method.

**Results**—The optimal OMI ischemic thresholds were found to be 0.28 and 0.42 of normal values in the contralateral hemisphere. Using the 10-fold cross-validation method, median infarct probabilities were 90.6% for core, 89.7% for non-reperfused penumbra, 9.95% for reperfused penumbra, and 6.28% for not-at-risk tissue.

**Conclusions**—OMI thresholds, derived using voxel-based, reperfusion-dependent infarct probabilities, delineated the ischemic penumbra with high predictive ability. These thresholds will require confirmation in an independent patient sample.

## Background and Purpose

Imaging the ischemic penumbra during hyperacute stroke has been actively investigated because of its potential to individualize therapeutic opportunities beyond population-defined time-windows. The ischemic penumbra was defined by Astrup<sup>1</sup> as “a zone of nonfunctioning but viable tissue that may recover its function if blood flow can be restored, for example, by therapeutic intervention.” This concept originated from electrophysiological studies in primates which revealed two cerebral blood flow (CBF) thresholds: a lower threshold of ion-pump failure that was associated with tissue infarction, and an upper threshold denoted by electrical failure, but associated with preserved tissue structure. The initial use of CBF thresholds to define the penumbra was problematic because the threshold delineating the ischemic core changed with increasing duration of ischemia.<sup>2</sup> Subsequent PET studies in animal models and in stroke patients demonstrated that as CBF dropped in the affected region, oxygen extraction fraction (OEF) increased in attempt to maintain tissue-level metabolism or cerebral metabolic rate of oxygen utilization ( $CMRO_2 = CBF \times OEF \times \text{arterial oxygen content}$ ). Despite elevation of OEF in the peri-infarct region, OEF alone was found to be a relatively weak predictor of tissue outcome,<sup>3</sup> whereas  $CMRO_2$  more consistently delineated tissue that eventually died<sup>4–6</sup> with thresholds for infarction ranging from 0.87–1.7 mL 100g<sup>-1</sup> min<sup>-1</sup>  $CMRO_2 < 23–55\%$  of normal values. Values at the lower end of the range were derived from single voxel measurements of both gray and white matter, whereas those at the higher end were determined from larger regions of interest primarily in gray matter.<sup>4, 7–11</sup> Unlike CBF thresholds,  $CMRO_2$  thresholds appeared independent of the time interval after stroke onset, making it ideal for imaging salvageable tissue in stroke patients who present at various times after stroke onset.<sup>12</sup>

Given the logistical hurdles of PET in hyperacute stroke patients, MR and CT methods have been actively explored. While initial studies of MR diffusion perfusion mismatch (DPM) and CT perfusion mismatch as a penumbral imaging signature were promising, clinical trials were unable to demonstrate improved clinical outcomes when selecting patients with DPM for therapy. The Echoplanar Imaging Thrombolytic Evaluation Trial (EPITHET) randomized patients to tPA vs. placebo between 3–6 hours from stroke onset.<sup>13</sup> Patients with DPM who were given tPA did not show significantly decreased infarct growth compared to placebo. The Desmoteplase in Acute Stroke (DIAS) -II trial did not demonstrate any benefit with a novel thrombolytic, desmoteplase, compared to placebo in

mismatch-selected patients.<sup>14</sup> MR RESCUE (Mechanical Retrieval and Recanalization of Stroke Clots Using Embolectomy) randomized patients to clot retrieval vs. medical therapy within 8 hours of onset and found no benefit from intervention in patients with penumbral pattern using mismatch criteria.<sup>15</sup> Further DPM trials are underway, to determine if optimized DPM thresholds will identify individuals who might benefit from acute interventions.

With the goal of finding a physiological biomarker of penumbral tissue, we developed an MR method capable of assessing cerebral oxygen metabolism termed MR-oxygen metabolic index (OMI).<sup>16</sup> This method has been validated in animal models subjected to hypoxia, hypercapnia, and middle cerebral artery occlusion against jugular venous oxygen saturation sampling.<sup>17</sup> In healthy subjects inhaling variable mixtures of carbogen, OMI yielded similar values to those found in PET studies with high reproducibility.<sup>18</sup> Furthermore, in a study of acute stroke patients, OMI values in the eventually infarcted region were  $0.40 \pm 0.24$  of the contralateral hemisphere, consistent with PET-derived CMRO<sub>2</sub> values for non-viable tissue.<sup>8</sup>

In this prospective imaging study, we tested OMI as a predictor of tissue fate in a cohort of acute ischemic stroke patients imaged within 4.5 hours of stroke symptom onset and re-imaged at 6 hours after stroke onset to assess reperfusion status. Using a voxel-by-voxel approach, our aim was to derive two quantitative ischemic thresholds for delineation of the ischemic penumbra: (1) a lower threshold of irreversible injury which differentiated ischemic core from penumbra and (2) an upper threshold of reversible injury which differentiated penumbra from oligemia. Consistent with Astrup's definition,<sup>1</sup> penumbra was defined based on reperfusion-dependent tissue survival: if reperfused, penumbral tissue should survive; if not reperfused, penumbral tissue should die.

## Methods

### Patients and Inclusion Criteria

Approval of the protocol was obtained from the Washington University Human Studies Committee. This was a prospective, observational MRI study in acute ischemic stroke patients at a large, urban, tertiary care referral center. There was no overlap of patients between the current study and previous reports of OMI. After providing written informed consent, both intravenous (IV) tPA-treated and untreated acute ischemic stroke patients with a National Institutes of Health Stroke Scale (NIHSS)  $\geq 5$  were enrolled (Supplementary Online Table for full inclusion and exclusion criteria). The study imposed no delay in time-to-tPA treatment and no deviation from standard monitoring practices. The NIHSS was collected prospectively by a stroke neurologist or stroke research coordinator on admission, at 72 hours, and at all imaging time points. Clinical data including demographic data and past medical history were obtained by the research coordinator prospectively at the time of patient enrollment.

## Magnetic Resonance Imaging Protocol

Patients underwent serial MRI scans at three time-points (tp): within 4.5 hours (tp1), at 6 hours (tp2), and at 1 month (tp3) after stroke onset, on a 3T Siemens whole body Trio. For patients receiving IV tPA, the tp1 scan was performed as soon as possible after tPA bolus (during tPA infusion). Six hours was chosen for the time of reperfusion measurement because reperfusion-based therapies administered within, but not beyond, this time-frame have demonstrated clinical efficacy.<sup>19, 20</sup> One month was chosen as the time for final infarct determination as stroke-related edema has diminished significantly by one month and atrophy may become significant beyond one month.<sup>21, 22</sup>

The protocol included diffusion-weighted, FLAIR [TR/TE=10000/115 ms; inversion time = 2500 ms; matrix=512×416; 20 slices, slice thickness (TH)=5mm], MPRAGE, and dynamic susceptibility contrast (DSC) perfusion images with 0.2ml/kg gadolinium contrast injected at 5 ml/sec (a T2\*-weighted gradient echo EPI sequence; TR/TE=1500/43ms; 14 slices, TH=5mm, zero interslice gap; matrix=128×128). The protocol did not include magnetic resonance angiography (MRA). The DSC method provided the perfusion weighted imaging (PWI) for calculation of CBF and cerebral blood volume (CBV) maps. Mean transit time (MTT) was calculated as CBV/CBF. Voxels within the proximal middle cerebral artery (MCA) of the contralateral hemisphere were manually chosen and the mean concentration curve of these voxels was used as the arterial input function (AIF). A time-shift insensitive block-circulant singular value decomposition method was utilized to minimize effects of time lag of the AIF on perfusion measurements.<sup>23</sup> To minimize large vessel effects which contribute to artifactually high signal near the cortical vertices, voxels with CBV > 10% of were removed and excluded from further analysis in deriving OMI thresholds for core, penumbra, and not-at-risk tissues (normal CBV for gray matter is 3–5% and for white matter is 1.5–3%). An asymmetric spin echo sequence was used to calculate OEF.<sup>24</sup> Oxygen metabolic index (OMI) was calculated as CBF × OEF. Measurements were normalized to the contralateral unaffected hemisphere. Detailed descriptions for quantification of OEF and OMI can be found elsewhere.<sup>24, 25</sup> MR-OEF images were acquired in 30 second epochs, so that those with significant motion artifact could be removed from the final signal-averaged OEF measure. If more than 10% of OEF images from a single time-point were removed due to motion, the patient was removed from the analysis.

Six parameter rigid image registration was performed to align all images across tp1, tp2, and tp3 for each patient using a well-established linear registration tool FSL 3.2 (FMRIB, Oxford, UK).<sup>26</sup> Accuracy of image registration was evaluated manually by a board-certified neuroradiologist (K.D.V.) who checked several structural landmarks, such as the ventricle and brain boundaries, in all registered images and their corresponding template image for each patient. If co-registration was found to be discrepant from the template image of more than 3 voxels in any direction, the registration algorithm was modified and rerun to improve alignment. Using this manual checking process, no patients who had all three imaging time-points were removed due to inadequate co-registration.

Tissue segmentation into gray and white matter, necessary for calculation of CBF and OMI prior to normalization with the contralateral hemisphere, was performed using a semi-automated approach using FSL 3.2 (FMRIB, Oxford, UK) for automatic segmentation<sup>26</sup>

followed by manual correction by a board-certified neuroradiologist (M.R.P.) using SNAP-ITK 2.2.0.<sup>27</sup> For delineation of the final infarct, hyperintense lesions were manually outlined on the 1 month FLAIR image by a board-certified vascular neurologist (A.L.F.) who was blinded to the OMI data. Each voxel on the 1 month FLAIR image was assigned a value of “dead” or “alive” for infarct probability analysis.

### Derivation of OMI Thresholds

All tp1 OMI voxels within the affected hemisphere were included for OMI threshold evaluation. Two OMI thresholds for delineating the ischemic penumbra were derived from the individual patient tp1 OMI maps based on a computation-intensive approach searching for the optimal threshold pair, which included: (1) a lower irreversible injury OMI threshold to distinguish the ischemic core from the ischemic penumbra and (2) an upper reversible injury OMI threshold to distinguish ischemic penumbra from tissue ‘not-at-risk’ for infarction. Specifically, a four-cell approach, reflecting four different tissue categories (core, non-reperfused penumbra, reperfused penumbra, and not-as-risk tissue) was employed. OMI threshold pairs were iteratively tested, searching for the threshold pair which resulted in infarct probabilities (IP) closest to ideal values in each tissue group of interest: (1) *core* (tissue died regardless of reperfusion), ideal IP=100%; (2) *non-reperfused\_penumbra* (tissue died without reperfusion), ideal IP=100%; (3) *reperfused\_penumbra* (tissue survived with reperfusion), ideal IP=0%; and (4) *not-as-risk tissue* (tissue survived regardless of reperfusion), ideal IP=0% (Figure 1). To this end, the threshold pair with the lowest “average prediction error (APE)”, a metric averaging the differences for each tissue group’s actual infarct probability from the ideal, was selected as optimal pair for delineating the penumbra. Therefore,  $APE = (|100\% - IP_{core}| + |100\% - IP_{non-reperfused\_penumbra}| + |0\% - IP_{reperfused\_penumbra}| + |0\% - IP_{not-at-risk}|) / 4$ . Threshold pairs were derived in individual patients and the median infarct probabilities and corresponding average prediction error were calculated for each pair. The pair with the lowest median average prediction error across the total sample was chosen as optimal. Hypoperfusion was defined in regions with MTT prolongation beyond the median MTT of the contralateral hemisphere ( $MTTp > 4$  seconds at tp1. “Reperfusion” within the penumbra was defined as  $MTTp < 4$  seconds at tp2 based on our previous analyses evaluating MTTp thresholds.<sup>28</sup> “Non-reperfusion” was defined as a voxel with an MTTp perfusion deficit  $> 4$  seconds at tp2. OMI threshold ranges (0.16–0.32 for irreversible-injury and 0.38–0.52 for reversible-injury in increments of 0.02) were chosen based on threshold ranges found within PET literature measuring  $CMRO_2$  in ischemic stroke patients.<sup>29</sup> To reduce noise-induced effects, a minimum volume of 1 ml for a tissue group was required to be included for average prediction error calculation.

### Cross-validation of OMI Thresholds

The predictive abilities of the derived OMI thresholds were tested in the same sample using a 10-fold cross-validation method.<sup>30</sup> The sample was partitioned into 10 equal subsamples. Of the 10 subsamples, 9 subsamples were used to derive the optimal ischemic thresholds. The derived thresholds were then tested on each of the patients within the one subsample left-out; average prediction error and the infarct probabilities for the tissue groups were calculated. This cross-validation process was repeated nine times, with each of the 10 subsamples used only once as the test subsample. Population-level infarct probabilities and

average prediction errors were displayed as median [25<sup>th</sup> quartile, 75<sup>th</sup> quartile]. Analyses were performed using Matlab v. R2012a.

## Results

Sixty-four patients who met all inclusion and exclusion criteria were consented and underwent tp1 imaging, of whom 24 patients were excluded due to: (1) inability to get tp2 due to medical instability, intolerance of tp1 MRI due to claustrophobia, or early reperfusion on tp1 imaging (N=7); (2) lost to follow-up or died prior to last imaging session (N=10); or (3) poor data quality due to motion artifact (N=7) (Supplemental Online Figure). Therefore, 40 patients were included in the final analysis. Baseline clinical and imaging characteristics for the 40 patients are shown in Table 1. These patients were imaged at a median of 2.7 hr (tp1), 6.3 hr (tp2), and 1 month (tp3) after stroke onset.

### Deriving the optimal OMI thresholds for delineating the penumbra

Putative OMI threshold pairs were used to define 3 tissue groups: core, penumbra, and not-at-risk. The putative penumbra was further subdivided by reperfusion status (non-reperfused penumbra and reperfused penumbra). Infarct probabilities were determined for each of these four tissue groups: core, non-reperfused penumbra, reperfused penumbra, and not-at-risk. Figure 2 shows an example from one patient, using the OMI threshold pair, 0.28 for irreversible injury and 0.42 for reversible injury. Infarct probabilities for this patient were 98.0% for core, 68.3% for non-reperfused penumbra, 9.8% for reperfused penumbra, and 1.1% for not-at-risk, yielding an “average prediction error” of 11.2%. The “average prediction error” is a value which describes the average deviation from ideal infarct probabilities (see Methods).

Using a computation-intensive search method, all possible threshold pairs within pre-defined ranges were applied to all patients, and infarct probabilities were calculated for each of the tissue groups. A median population average prediction error was calculated for each threshold pair. A matrix of threshold pairs with its corresponding median average prediction error values was created and displayed as a 3-D graph (Figure 3). The ideal threshold pair was defined as the pair with the lowest average prediction error value, indicating the lowest deviation from ideal prediction of tissue outcome. A single threshold pair was found to have the lowest average prediction error from the patient population, corresponding to an OMI threshold of 0.28 for irreversible injury and 0.42 for reversible injury (Figure 3, \*). This optimal threshold pair yielded an average prediction error of 8.75%, corresponding to the following infarct probabilities: (1) 92.9% [61.5, 97.6] for core, 92.2% [77.3, 96.4] for non-reperfused penumbra, 9.95% [0.30, 28.5] for reperfused penumbra, and 6.28% [1.72, 14.0] for not-at-risk tissue.

### Testing the predictive ability of OMI thresholds

The 10-fold cross-validation method produced thresholds ranging from 0.24–0.28 for the irreversible injury threshold and from 0.42–0.44 for the reversible injury threshold for the 10 subsample derivation sets. The 10 subsample threshold data is shown in Table 2. The median infarct probabilities in the 10 subsample test sets were: 90.6% [61.5, 97.7] for core,

89.7% [78.0, 95.2] for non-reperfused penumbra, 9.95% [0.33, 28.2] for reperfused penumbra, and 6.28% [1.72, 14.0] for not-at-risk tissue, corresponding to an average prediction error of 11.4% [2.69, 21.0] (Table 3).

## Discussion

In this prospective imaging study, a novel MR parameter designed to measure cerebral oxygen metabolism (OMI) was tested to determine if it could accurately delineate the ischemic penumbra. Two optimal OMI thresholds were identified which delineated core, penumbra, and oligemic tissue, and yielded reperfusion-dependent infarct probabilities close to ideal predicted tissue fate. Penumbra infarct probabilities within each voxel of tissue were strictly defined by reperfusion status: the ideal infarct probability was 0% if reperfused and 100% if not reperfused. Moreover, when the optimal thresholds were tested using the cross-validation technique, thresholds demonstrated little variability and yielded median infarct probabilities that were near ideal, suggesting that the derived thresholds were highly predictive of ideal tissue fate across the population.

The current study has several strengths: (1) our definition of penumbra was based on the definition by Astrup,<sup>1</sup> as operationalized by others,<sup>5</sup> requiring that reperfused voxels between the two optimal thresholds have low infarct probability and non-reperfused voxels have high infarct probability; (2) the timing of reperfusion measurement at six hours was chosen specifically to be within a time window known to impact clinical outcome in previous stroke populations;<sup>19, 31</sup> we aimed to define the OMI thresholds based on clinically-relevant reperfusion that would truly salvage tissue;<sup>28</sup> (3) we used a novel, unbiased approach to derive ischemic thresholds by employing a computation-intensive search method to minimize average prediction error; and (4) a voxel-wise approach was utilized for all analyses: all definitions were applied to co-registered voxels at three time-points, rather than visual, regional, or volumetric analyses.<sup>13, 14, 32</sup>

In the current study, we derived OMI thresholds for a time window in which reperfusion-promoting therapies are known to improve outcomes; however, future studies will test these thresholds at later windows. PET data suggests the CMRO<sub>2</sub> threshold delineating tissue outcome may be independent of time from symptom onset.<sup>12, 29</sup> This theory of time-independence is based on independent studies which have measured CMRO<sub>2</sub> at different time-points and arrived at a similar threshold for delineating tissue with eventual infarction; however, this threshold has not been tested for time-independence within a single study. Therefore, it will be important to determine if the OMI thresholds derived in this study will predict reperfusion-based tissue fate at later time windows.

A challenge with clinical trials thus far has been defining penumbral thresholds, which have largely been chosen empirically.<sup>13, 14, 33</sup> In early DPM trials, the reversible injury threshold (using a PWI-based parameter to separate penumbra from oligemia) was found to encompass significant oligemic tissue that was not at true risk for eventual infarction.<sup>13, 33</sup> Post-hoc analyses helped to refine the optimal thresholds for use in subsequent studies.<sup>15, 34-36</sup> More recently, MR-RESCUE investigators rigorously derived the threshold for irreversibly-injury by developing a multi-parametric model (including DWI and PWI

parameters) to predict the infarct core in the setting of successful recanalization.<sup>37</sup> The threshold for reversible injury was not optimized, but was empirically chosen. To build upon these methods, we aimed to prospectively identify the best-performing, quantitative penumbral thresholds for both irreversible and reversible injury so that the optimal thresholds would be known if tested within the context of a clinical trial.

This study has several limitations. 1) Data was obtained from a single institution; therefore, the generalizability of thresholds to other populations is unknown. 2) Inclusion criteria required NIHSS  $\geq 5$ ; therefore, this cohort captured strokes of greater severity (median NIHSS=14) than average stroke patients. 3) Because the first imaging session occurred, on average, 46 minutes after tPA treatment, some tissue that was initially ischemic might have been lost to analysis due to early reperfusion. 4) Tissue (gray-white matter) segmentation is required for calculating normalized OMI. Therefore, prior to implementation in clinical practice, a rapid processing algorithm will need to be developed, similar to current rapid post-processing tools used for diffusion-perfusion mismatch.<sup>38</sup> 5) We assessed the reproducibility and predictive ability of the OMI thresholds on the same patient cohort in which the thresholds were derived using a statistical resampling method. Therefore, the thresholds will need to be tested in an independent population. 6) The clinical utility of OMI ischemic thresholds will need to be tested to evaluate how much OMI-defined penumbral tissue is required to yield meaningful clinical benefit and whether OMI promotes the efficacy of an intervention by appropriately selecting patients for therapy. 7) Finally, we are directly comparing MR-OMI values to PET derived CMRO<sub>2</sub> values in patients with cerebrovascular disease in an ongoing study, which will permit further refinement of MR-OMI.

## Conclusion

OMI ischemic thresholds, derived using voxel-based final infarct and reperfusion status, delineated the ischemic penumbra with high predictive ability and were consistent when retested within the population. These thresholds will require further testing in independent patient cohorts.

## Supplementary Material

Refer to Web version on PubMed Central for supplementary material.

## Acknowledgments

We are grateful to the stroke research coordinators and emergency department staff for the help with patient enrollment.

**Sources of Funding:** This study was supported by grants from National Institute of Health NIH 5P50NS055977 (to JML, CPD, WJP, and HA) and K23 NS069807 (to AF) and from the Washington University Institute of Clinical and Translational Sciences grant UL1 TR000448 from the National Center for Advancing Translational Sciences of the National Institutes of Health.



## References

1. Astrup J. Energy-requiring cell functions in the ischemic brain. Their critical supply and possible inhibition in protective therapy. *Journal of neurosurgery*. 1982; 56:482–497. [PubMed: 6278105]
2. Jones TH, Morawetz RB, Crowell RM, Marcoux FW, FitzGibbon SJ, DeGirolami U, et al. Thresholds of focal cerebral ischemia in awake monkeys. *Journal of neurosurgery*. 1981; 54:773–782. [PubMed: 7241187]
3. Young AR, Sette G, Touzani O, Rioux P, Derlon JM, MacKenzie ET, et al. Relationships between high oxygen extraction fraction in the acute stage and final infarction in reversible middle cerebral artery occlusion: An investigation in anesthetized baboons with positron emission tomography. *J Cereb Blood Flow Metab*. 1996; 16:1176–1188. [PubMed: 8898690]
4. Heiss WD, Huber M, Fink GR, Herholz K, Pietrzyk U, Wagner R, et al. Progressive derangement of periinfarct viable tissue in ischemic stroke. *J Cereb Blood Flow Metab*. 1992; 12:193–203. [PubMed: 1548292]
5. Furlan M, Marchal G, Viader F, Derlon JM, Baron JC. Spontaneous neurological recovery after stroke and the fate of the ischemic penumbra. *Ann Neurol*. 1996; 40:216–226. [PubMed: 8773603]
6. Wise RJ, Bernardi S, Frackowiak RS, Legg NJ, Jones T. Serial observations on the pathophysiology of acute stroke. The transition from ischaemia to infarction as reflected in regional oxygen extraction. *Brain*. 1983; 106(Pt 1):197–222. [PubMed: 6600956]
7. Giffard C, Young AR, Kerrouche N, Derlon JM, Baron JC. Outcome of acutely ischemic brain tissue in prolonged middle cerebral artery occlusion: A serial positron emission tomography investigation in the baboon. *J Cereb Blood Flow Metab*. 2004; 24:495–508. [PubMed: 15129181]
8. Powers WJ, Grubb RL Jr, Darriet D, Raichle ME. Cerebral blood flow and cerebral metabolic rate of oxygen requirements for cerebral function and viability in humans. *J Cereb Blood Flow Metab*. 1985; 5:600–608. [PubMed: 3877067]
9. Touzani O, Young AR, Derlon JM, Baron JC, MacKenzie ET. Progressive impairment of brain oxidative metabolism reversed by reperfusion following middle cerebral artery occlusion in anaesthetized baboons. *Brain Res*. 1997; 767:17–25. [PubMed: 9365011]
10. Touzani O, Young AR, Derlon JM, Beaudouin V, Marchal G, Rioux P, et al. Sequential studies of severely hypometabolic tissue volumes after permanent middle cerebral artery occlusion. A positron emission tomographic investigation in anesthetized baboons. *Stroke*. 1995; 26:2112–2119. [PubMed: 7482659]
11. Baron JC, Bouser MG, Lebrun-Grandie P, Iba-Zizen MT, Chiras J. Local CBF, oxygen extraction fraction (OEF), and CMRO<sub>2</sub>: Prognostic value in recent supratentorial infarction in humans. *J Cereb Blood Flow Metab*. 1983; 3:S1–S2. [PubMed: 6546215]
12. Baron JC, Marchal G. How time dependent is the threshold for cerebral infarction? *Stroke; a journal of cerebral circulation*. 1996; 27:1918–1919.
13. Davis SM, Donnan GA, Parsons MW, Levi C, Butcher KS, Peeters A, et al. Effects of alteplase beyond 3 h after stroke in the echoplanar imaging thrombolytic evaluation trial (EPITHET): A placebo-controlled randomised trial. *Lancet Neurol*. 2008; 7:299–309. [PubMed: 18296121]
14. Hacke W, Furlan AJ, Al-Rawi Y, Davalos A, Fiebich JB, Gruber F, et al. Intravenous desmoteplase in patients with acute ischaemic stroke selected by mri perfusion-diffusion weighted imaging or perfusion ct (DIAS-2): A prospective, randomised, double-blind, placebo-controlled study. *Lancet Neurol*. 2009; 8:141–150. [PubMed: 19097942]
15. Furlan AJ, Eyding D, Albers GW, Al-Rawi Y, Lees KR, Rowley HA, et al. Dose escalation of desmoteplase for acute ischemic stroke (DEDAS): Evidence of safety and efficacy 3 to 9 hours after stroke onset. *Stroke*. 2006; 37:1227–1231. [PubMed: 16574922]
16. Jensen-Kondering U, Baron JC. Oxygen imaging by mri: Can blood oxygen level-dependent imaging depict the ischemic penumbra? *Stroke*. 2012; 43:2264–2269. [PubMed: 22588263]
17. An H, Liu Q, Chen Y, Lin W. Evaluation of mr-derived cerebral oxygen metabolic index in experimental hyperoxic hypercapnia, hypoxia, and ischemia. *Stroke*. 2009; 40:2165–2172. [PubMed: 19359642]
18. Heiss WD. Experimental evidence of ischemic thresholds and functional recovery. *Stroke*. 1992; 23:1668–1672. [PubMed: 1440719]

19. Furlan A, Higashida R, Wechsler L, Gent M, Rowley H, Kase C, et al. Intra-arterial prourokinase for acute ischemic stroke. The PROACT II study: A randomized controlled trial. Prolyse in acute cerebral thromboembolism. *Jama*. 1999; 282:2003–2011. [PubMed: 10591382]
20. Powers WJ. Thrombolysis for acute ischemic stroke: Is intra-arterial better than intravenous? A treatment effects model. *Journal of stroke and cerebrovascular diseases : the official journal of National Stroke Association*. 2012; 21:401–403. [PubMed: 22464277]
21. Chemmanur T, Campbell BC, Christensen S, Nagakane Y, Desmond PM, Bladin CF, et al. Ischemic diffusion lesion reversal is uncommon and rarely alters perfusion-diffusion mismatch. *Neurology*. 75:1040–1047. [PubMed: 20720188]
22. Gaudinski MR, Henning EC, Miracle A, Luby M, Warach S, Latour LL. Establishing final infarct volume: Stroke lesion evolution past 30 days is insignificant. *Stroke; a journal of cerebral circulation*. 2008; 39:2765–2768.
23. Wu O, Ostergaard L, Weisskoff RM, Benner T, Rosen BR, Sorensen AG. Tracer arrival timing-insensitive technique for estimating flow in mr perfusion-weighted imaging using singular value decomposition with a block-circulant deconvolution matrix. *Magn Reson Med*. 2003; 50:164–174. [PubMed: 12815691]
24. An H, Lin W. Impact of intravascular signal on quantitative measures of cerebral oxygen extraction and blood volume under normo- and hypercapnic conditions using an asymmetric spin echo approach. *Magnetic resonance in medicine : official journal of the Society of Magnetic Resonance in Medicine / Society of Magnetic Resonance in Medicine*. 2003; 50:708–716.
25. Lee JM, Vo KD, An H, Celik A, Lee Y, Hsu CY, et al. Magnetic resonance cerebral metabolic rate of oxygen utilization in hyperacute stroke patients. *Ann Neurol*. 2003; 53:227–232. [PubMed: 12557290]
26. Jenkinson M, Smith S. A global optimisation method for robust affine registration of brain images. *Medical image analysis*. 2001; 5:143–156. [PubMed: 11516708]
27. Yushkevich PA, Piven J, Hazlett HC, Smith RG, Ho S, Gee JC, et al. User-guided 3d active contour segmentation of anatomical structures: Significantly improved efficiency and reliability. *NeuroImage*. 2006; 31:1116–1128. [PubMed: 16545965]
28. Warach S, Al-Rawi Y, Furlan AJ, Fiebach JB, Wintermark M, Lindsten A, et al. Refinement of the magnetic resonance diffusion-perfusion mismatch concept for thrombolytic patient selection: Insights from the desmoteplase in acute stroke trials. *Stroke*. 2012; 43:2313–2318. [PubMed: 22738918]
29. Zazulia, AR.; Markam, J.; Powers, WJ. Cerebral blood flow and metabolism in human cerebrovascular disease. In: Mohr, JP.; Wolf, PA., editors. *Stroke: Pathophysiology, Diagnosis, and Management*. Philadelphia, PA: Elsevier Saunders; 2011. p. 44-67.
30. Ambrose C, McLachlan GJ. Selection bias in gene extraction on the basis of microarray gene-expression data. *Proceedings of the National Academy of Sciences of the United States of America*. 2002; 99:6562–6566. [PubMed: 11983868]
31. Khatri P, Abruzzo T, Yeatts SD, Nichols C, Broderick JP, Tomsick TA, et al. Good clinical outcome after ischemic stroke with successful revascularization is time-dependent. *Neurology*. 2009; 73:1066–1072. [PubMed: 19786699]
32. Nagakane Y, Christensen S, Brekenfeld C, Ma H, Churilov L, Parsons MW, et al. EPITHET: Positive result after reanalysis using baseline diffusion-weighted imaging/perfusion-weighted imaging co-registration. *Stroke; a journal of cerebral circulation*. 2011; 42:59–64.
33. Albers GW, Thijs VN, Wechsler L, Kemp S, Schlaug G, Skalabrin E, et al. Magnetic resonance imaging profiles predict clinical response to early reperfusion: The diffusion and perfusion imaging evaluation for understanding stroke evolution (DEFUSE) study. *Ann Neurol*. 2006; 60:508–517. [PubMed: 17066483]
34. Lansberg MG, Straka M, Kemp S, Mlynash M, Wechsler, et al. DEFUSE 2 study investigators. MRI profile and response to endovascular reperfusion after stroke (DEFUSE 2): A prospective cohort study. *Lancet Neurology*. 2013; 11:860–867. [PubMed: 22954705]
35. Zaro-Weber O, Moeller-Hartmann W, Heiss WD, Sobesky J. Mri perfusion maps in acute stroke validated with 15o-water positron emission tomography. *Stroke*. 2010; 41:443–449. [PubMed: 20075355]

36. Takasawa M, Jones PS, Guadagno JV, Christensen S, Fryer TD, Harding S, et al. How reliable is perfusion mr in acute stroke? Validation and determination of the penumbra threshold against quantitative pet. *Stroke*. 2008; 39:870–877. [PubMed: 18258831]
37. Kidwell CS, Wintermark M, De Silva DA, Schaewe TJ, Jahan R, Starkman S, et al. Multiparametric MRI and CT models of infarct core and favorable penumbral imaging patterns in acute ischemic stroke. *Stroke*. 2013; 44:73–79. [PubMed: 23233383]
38. Lansberg MG, Lee J, Christensen S, Straka M, De Silva DA, Mlynash M, et al. Rapid automated patient selection for reperfusion therapy: A pooled analysis of the echoplanar imaging thrombolytic evaluation trial (EPITHET) and the diffusion and perfusion imaging evaluation for understanding stroke evolution (DEFUSE) study. *Stroke*. 2011; 42:1608–1614. [PubMed: 21493916]

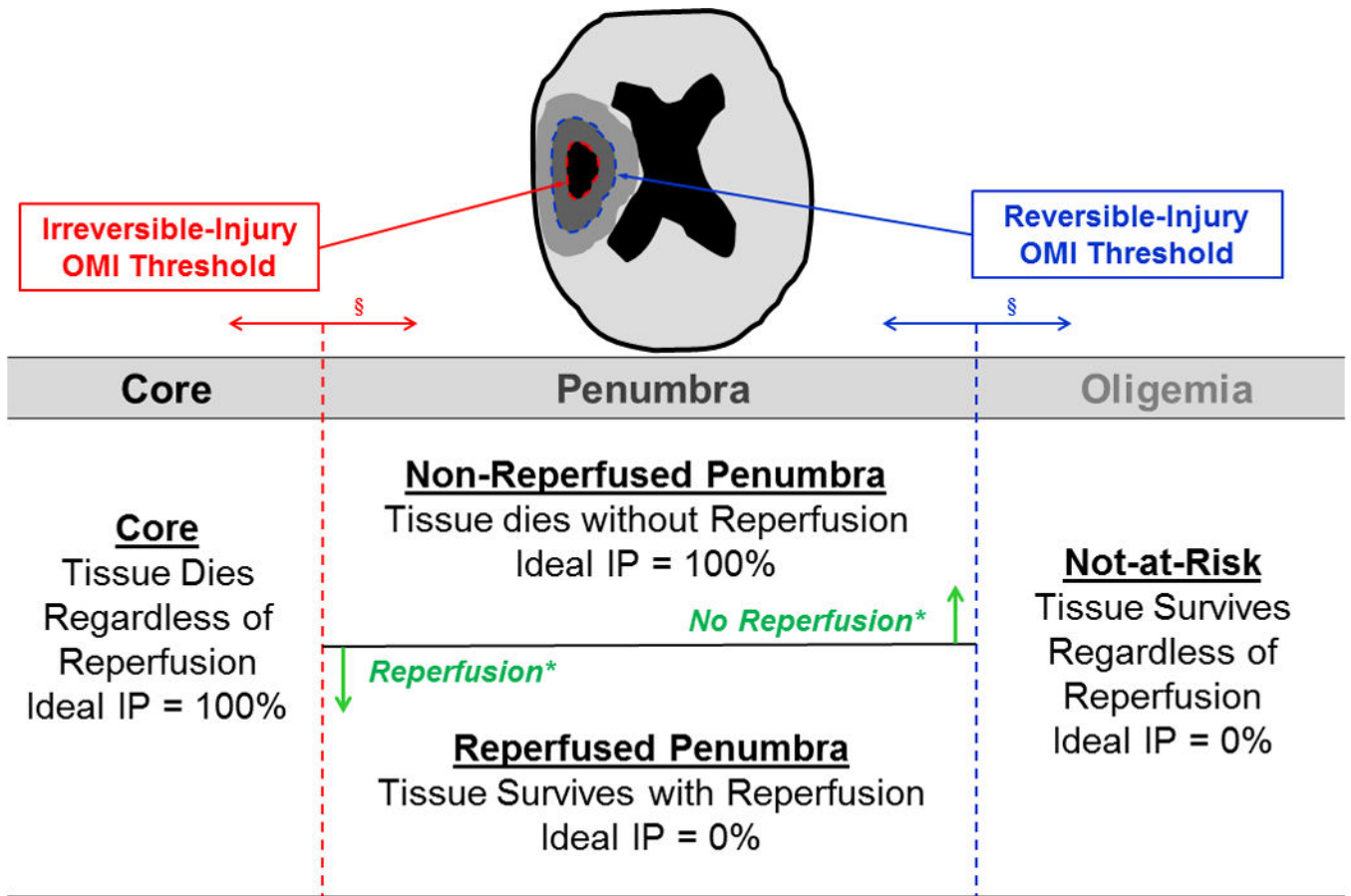


**Figure 1. Deriving OMI Penumbral Thresholds**

§Irreversible-injury and reversible-injury OMI threshold pairs separated the tissue within the ischemic hemisphere into core, penumbra, and not-at-risk; penumbra was further subdivided by reperfusion status (non-reperused penumbra and reperused penumbra). For each pair, the infarct probability (IP) from each tissue group was calculated. A computation-intensive search method was performed to find the OMI threshold pair that corresponded to the lowest average prediction error (a metric averaging the differences of the actual infarct probabilities from ideal infarct probabilities for all tissue groups). Average prediction error (APE) =  $\{|100\% - IP_{\text{core}}| + |100\% - IP_{\text{nonreperused\_penumbra}}| + |0\% - IP_{\text{reperused\_penumbra}}| + |0\% - IP_{\text{not-at-risk}}|\} / 4$ ; Ideal APE=0%. Pairs of irreversible and reversible-injury thresholds were iteratively tested and infarct probabilities in each of the four tissue groups and the corresponding average prediction error were calculated. The threshold pair with the lowest average prediction error was selected as the pair of optimal OMI thresholds.

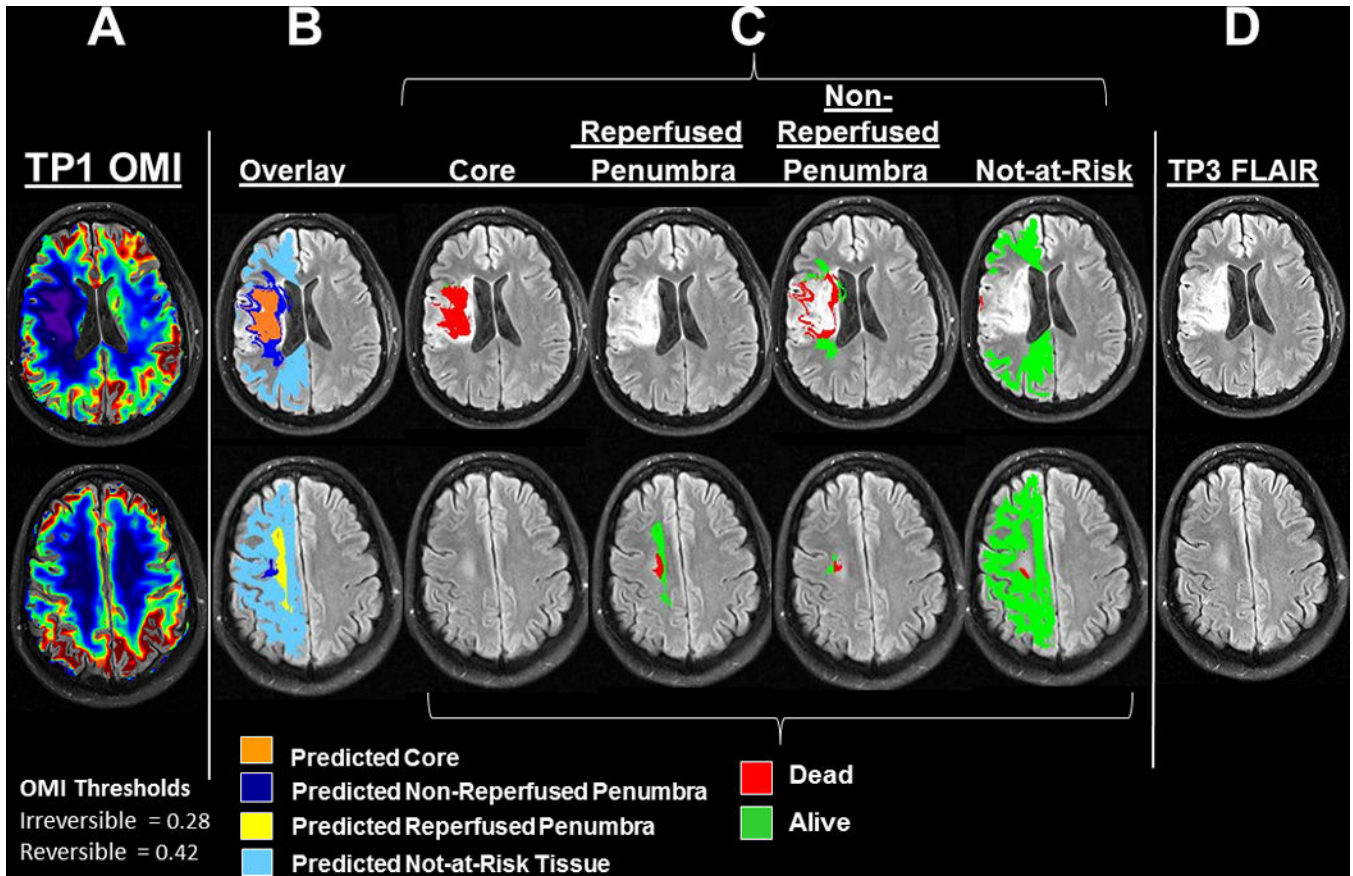


**Figure 2. Patient Example**

A 27 year old man with a right middle cerebral artery stroke (NIHSS=16) underwent tp1 MRI at 2:10 after symptom onset (during tPA infusion) followed by tp2 MRI at 6:28 after onset. Using tp1 OMI map (Column A), an example OMI threshold pair (core/penumbra=0.28, penumbra/not-at-risk=0.42) divided the tissue into predicted core, penumbra, and not-at-risk; penumbra was further subdivided based on reperfusion status (determined by tp2 scan) (Column B). For each of the four tissue groups (C), tissue that died (red) or survived (green) was determined based on the infarct delineated on FLAIR imaging at 1 month (Column D). The actual infarct probabilities from each group were calculated and subtracted from the ideal infarct probabilities, from which the average prediction error for this threshold pair in this patient was calculated.

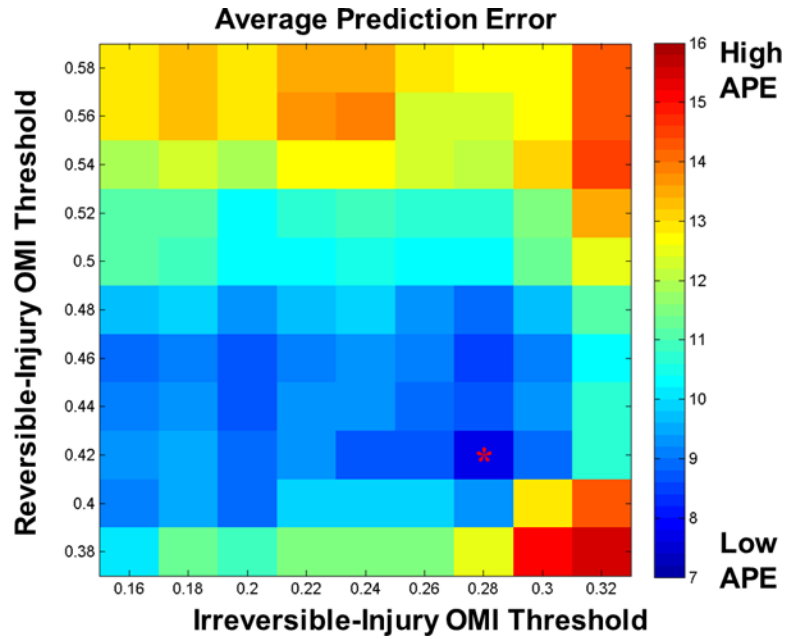


**Figure 3. Population-derived Average Prediction Errors as a function of varying the OMI Core/ Penumbra and Penumbra/Not-at-Risk Threshold Pairs**

A 3-D matrix of OMI threshold pairs with the corresponding median average prediction error values was plotted. The irreversible injury OMI threshold is on the x-axis. The reversible injury OMI threshold is on the y-axis. The average prediction error (APE) is on the color scale (in-plane) axis with cool colors representing the lowest average prediction error (closest to ideal) and warm colors representing the highest average prediction error (farthest from ideal). The ideal threshold pair was defined as the pair with the lowest average prediction error value, indicating the lowest deviation from ideal tissue outcome. The lowest single minimum average prediction error (8.75%) is found at the dark-blue square (\*) corresponding to an irreversible injury threshold of 0.28 and a reversible injury threshold of 0.42.

**Table 1**

## Patient Characteristics (N=40)

Female, n (%)	14 (35%)
Age (years)	64 [57, 72]
Admission NIHSS	14 [8, 19]
African-American, n (%)	14 (35%)
tPA treatment, n (%)	30 (75%)
Admission Mean Arterial Pressure (mmHg)	114 [106, 128]
Admission Glucose (mg/dl)	126 [107, 149]
Time to tp1, hour	2.7 [2.1, 3.5]
Time to tp2, hour	6.3 [6.1, 6.5]
History of Hypertension, n (%)	31 (78%)
History of Diabetes, n (%)	11 (28%)
History of Congestive Heart Failure, n (%)	5 (12%)
Current Tobacco Use, n (%)	12 (30%)
History of Coronary Artery Disease, n (%)	12 (30%)
History of Stroke or TIA, n (%)	8 (20%)

Continuous data shown as median [interquartile range]; NIHSS = National Institutes of Health Stroke Scale; tp1=time-point 1 MRI; tp2=time-point 2 MRI; TIA=transient ischemic attack

**Table 2**

Cross-validation Results for the Optimal OMI Thresholds in the 10 Subsamples

Subsample #	Irreversible-Injury OMI Threshold	Reversible-Injury OMI Threshold
1	0.28	0.42
2	0.28	0.42
3	0.28	0.42
4	0.24	0.42
5	0.28	0.42
6	0.28	0.42
7	0.28	0.42
8	0.28	0.42
9	0.26	0.44
10	0.28	0.42

Author Manuscript

Author Manuscript

Author Manuscript

Author Manuscript



**Table 3**

OMI Threshold 10-Fold Cross-Validation: Population-derived Median Infarct Probabilities and Average Prediction Error

	Core IP	Penumbra IPs	Not-at-Risk IP
Non-Reperfusion	90.6% [61.5, 97.7]	89.7% [78.0, 95.2]	6.28% [1.72, 14.0]
Reperfusion		9.95% [0.33, 28.2]	
<b>APE<sup>†</sup> = 11.4% [2.69, 21.0]</b>			

IP=Infarct Probability; Data shown as Median [25<sup>th</sup> quartile, 75<sup>th</sup> quartile].

<sup>†</sup> APE (Average Prediction Error) =  $(|100\% - IP_{core}| + |100\% - IP_{non-reperfusion\_penumbra}| + |0\% - IP_{reperfusion\_penumbra}| + |0\% - IP_{not-at-risk}|) / 4$ ; Ideal APE = 0%.